INTERNATIONAL JOURNAL FOR NUMERICAL METHODS IN ENGINEERING
Int. J. Numer. Meth. Engng 2006; **66**:2064–2085
Published online 13 January 2006 in Wiley InterScience (www.interscience.wiley.com). DOI: 10.1002/nme.1617

Truncation error in mesh-free particle methods

N. J. Quinlan*, †, M. Basa and M. Lastiwka

Department of Mechanical and Biomedical Engineering, National University of Ireland, Galway, Ireland

SUMMARY

A truncation error analysis has been developed for the approximation of spatial derivatives in smoothed particle hydrodynamics (SPH) and related first-order consistent methods such as the first-order form of the reproducing kernel particle method. Error is shown to depend on both the smoothing length h and the ratio of particle spacing to smoothing length, $\Delta x/h$. For uniformly spaced particles in one dimension, analysis shows that as h is reduced while maintaining constant $\Delta x/h$, error decays as h^2 until a limiting discretization error is reached, which is independent of h. If $\Delta x/h$ is reduced while maintaining constant h (i.e. if the number of neighbours per particle is increased), error decreases at a rate which depends on the kernel function's smoothness. When particles are distributed non-uniformly, error can grow as h is reduced with constant $\Delta x/h$. First-order consistent methods are shown to remove this divergent behaviour. Numerical experiments confirm the theoretical analysis for one dimension, and indicate that the main results are also true in three dimensions. This investigation highlights the complexity of error behaviour in SPH, and shows that the roles of both h and $\Delta x/h$ must be considered when choosing particle distributions and smoothing lengths. Copyright © 2005 John Wiley & Sons, Ltd.

KEY WORDS: smoothed particle hydrodynamics; meshfree methods; meshless methods; particle methods; error analysis

1. INTRODUCTION

In this paper, a new investigation of truncation error is presented for smoothed particle hydrodynamics (SPH) and related numerical methods. SPH is a mesh-free Lagrangian technique for the solution of partial differential equations in computational mechanics. It was created by Lucy [1] and Monaghan and Gingold [2] for use in astrophysics, and subsequently found application in solid impact and fracture problems, and in fluid mechanics. Comprehensive

*Correspondence to: N. J. Quinlan, Department of Mechanical and Biomedical Engineering, National University of Ireland, Galway, Ireland.
†E-mail: nathan.quinlan@nuigalway.ie

Contract/grant sponsor: Irish Research Council for Science, Engineering and Technology; contract/grant number: SC/02/189

Received 17 August 2005
Revised 12 November 2005
Accepted 14 November 2005

Copyright © 2005 John Wiley & Sons, Ltd.

reviews of the method are available in articles by Monaghan [3–5], Randles and Libersky [6] and Vignjevic [7], and the texts by Li and Liu [8] and Liu and Liu [9]. The attractions of meshfree particle methods for fluid dynamics include the ease of dealing with multiphase flow and moving walls in the Lagrangian framework, as well as elimination of the mesh. In recent years there has been significant progress towards industrial application for fluid dynamics, with extensions to incompressible flow [10–13], viscous flow [14–16], and turbulence modelling both by Reynolds-averaged Navier–Stokes methods and large eddy simulation [17, 18].

SPH is based on an approximation which allows the value of a function and its gradients to be estimated at an arbitrary location, given function values at arbitrary unconnected data points. In simulation of physical phenomena, these points move at local material velocity and possess mass and other physical properties, and are therefore called particles. The SPH approximation to the gradient of a function $A(\mathbf{x})$ at a particle a is

$$\nabla A(\mathbf{x})|_{\mathbf{x}=\mathbf{x}_a} \approx \int \nabla A(\mathbf{x}) W(\mathbf{x}-\mathbf{x}_a, h)\,\mathrm{d}V = -\int A(\mathbf{x}) \nabla W(\mathbf{x}-\mathbf{x}_a, h)\,\mathrm{d}V$$

$$\approx -\sum_b A(\mathbf{x}_b) \nabla W(\mathbf{x}-\mathbf{x}_a, h)|_{\mathbf{x}=\mathbf{x}_b} \Delta V_b \tag{1}$$

Here, $W(\mathbf{x}-\mathbf{x}_a, h)$ is a kernel function which tends to zero with increasing distance between $\mathbf{x}$ and $\mathbf{x}_a$, and is usually designed with a maximum at $\mathbf{x}=\mathbf{x}_a$. h is a parameter known as the smoothing length or dilation parameter, which characterizes the radius over which the kernel decays. Most kernels described in the literature have compact support—that is, they are zero-valued at all locations beyond a finite distance from the central point. In this work, as in most of the literature, the smoothing length h is defined as half the compact support radius. Integrals in Equation (1) are taken over the whole domain, or the compact support.

The summation is taken over all particles b within the compact support for the point $\mathbf{x}_a$. The particle volume ΔV_b acts as a weighting on the contribution of particle b to the sum. In practice, ΔV_b is often calculated as the ratio of mass to density, m_b/ρ. The above equation is the 'gather' formulation of SPH, in which the kernel is considered to be centred at particle a, where the approximation is to be evaluated. As Equation (1) suggests, it is useful (but by no means essential) to interpret SPH as a discrete approximation to a continuous smoothing approximation to the true gradient.

Inspection of Equation (1) shows that SPH does not possess zero-order consistency. In other words, in general, it will not exactly estimate the first derivative of a zero-order polynomial (constant-valued) function. However, several related methods do possess consistency properties [8]. The reproducing kernel particle method (RKPM) due to Liu *et al.* [19], moving least squares particle hydrodynamics of Dilts [20] and corrected SPH of Bonet and Lok [21] are all at least first-order consistent. Liu *et al.* [22] showed how to construct a method of arbitrary consistency order. Any of these consistent particle methods can be represented by Equation (1) with the appropriate definition for the kernel function, or in the correction devised by Bonet and Lok, with a modification to the ∇ operator.

Particle methods for computational mechanics are assembled by replacing gradients in the governing partial differential equations with approximations such as Equation (1). Governing PDEs which feature material time derivatives benefit from the Lagrangian treatment, as convective and local time derivatives can be lumped into a single time derivative following each particle. The accuracy of the simulation depends on the accuracy of the underlying

Copyright © 2005 John Wiley & Sons, Ltd.

approximation to spatial derivatives; however, the nature of error is not understood as well for these methods as for their mesh-based counterparts. By considering the continuous, integral form of SPH, Monaghan [3] and others have noted that the SPH interpolation is accurate to second order in h, and that fourth-order accuracy can be achieved with special kernel functions. This type of analysis does not account for the discrete character of the method. Meglicki [23] considered the accuracy of the discrete approximation in smoothed particle magnetohydrodynamics and determined guidelines for particle number density. Fulk and Quinn [24] showed that 1D standard SPH can model quadratic functions exactly for certain values of particle spacing, and derived a figure of merit to aid SPH users in selection of a kernel. Cleary and Monaghan [25] emphasized the importance of particle spacing in the context of a thermal conduction problem. They suggested that if particle spacing Δx is reduced more quickly than smoothing length h, overall error would be of order h^2. In numerical experiments, they demonstrated second-order convergence while maintaining a fixed ratio of particle spacing to smoothing length. Han and Meng [26] have shown theoretically that error in RKPM is of order h^{p+1} for certain classes of particle distribution and data function, where p is the highest order of polynomial function to be reproduced exactly.

Despite these important results, it remains difficult to make simple general statements about the accuracy of SPH and related methods. It is not clear on theoretical grounds how the second-order accuracy noted by many authors for the continuous smoothing stage translates into the full discrete form. Little practical information is available about the influence of particle spacing on errors. In this paper two direct approaches are used to move towards answers to these important questions of accuracy. Truncation error of the gradient estimate is investigated analytically using Taylor series expansions, and numerical experiments are conducted to determine the error in evaluation of gradients of known data functions.

The investigation begins with the special cases of standard SPH approximations in one dimension for uniform (Section 3.1) and non-uniform (Section 3.2) particle distributions. Corrected 1D SPH methods are considered in Section 4. Accuracy of standard and corrected methods in 3D is discussed in Section 5. Theoretical analysis and numerical experiments complement each other throughout the study, although the theoretical treatment for three dimensions is limited. In Section 6, the results are discussed in terms of the convergence of mesh-free particle methods in practical scenarios.

2. KERNEL FUNCTIONS

2.1. Construction and properties of kernel functions

In early SPH research [2], a Gaussian kernel function defined by Equation (2) was widely used.

$$W_G(r_a, h) = \frac{1}{h\sqrt{\pi}} \mathrm{e}^{-(r_a/h)^2} \tag{2}$$

(All of the kernels described in this section are defined in their one-dimensional form for simplicity; they can easily be adapted to two or three dimensions by scaling to meet the normalization requirement, which is discussed in Sections 2.2 and 3.) $r_a = |\mathbf{x} - \mathbf{x}_a|$ is defined as the distance from the particle of interest, a. The Gaussian kernel has infinite support, so that every particle interacts with every other particle in the domain, and computational cost rises rapidly with the number of particles. Infinite support is questionable in modelling compressible

Copyright © 2005 John Wiley & Sons, Ltd.

flow, in which information propagates at finite speed. (Conversely, it could be argued that incompressible flows should be modelled with infinite support, as the speed of sound is infinite and information propagates instantaneously throughout the field. In practice, however, some researchers have modelled incompressible flow with compact support kernels by using a large but finite speed of sound [10]. Other approaches involve solution of a global equation system, which results in instantaneous information propagation throughout the domain, regardless of the kernel support radius [11–13].)

The cubic B-spline defined by Equation (3) [27] later became a popular choice.

$$W_B(r_a, h) = \frac{2}{3h} \begin{cases} 1 - \frac{3}{2}\left(\frac{r_a}{h}\right)^2 + \frac{3}{4}\left(\frac{r_a}{h}\right)^3, & \frac{r_a}{h} < 1 \\ \frac{1}{4}\left(2 - \frac{r_a}{h}\right)^3, & 1 \leqslant \frac{r_a}{h} < 2 \\ 0, & \frac{r_a}{h} \geqslant 2 \end{cases} \tag{3}$$

This is a piecewise cubic function with compact support on a radius $2h$, where h is the smoothing length. It has discontinuities in its third derivative at $(x - x_a)/h = 0, \pm 1, \pm 2$ (in one dimension). The kernel value and its first and second derivatives are zero at the edges of the compact support. Higher-order spline kernels have also been described in the literature [28].

Boundary smoothness of a kernel function is defined for the purposes of this analysis as the highest integer β such that the βth derivative and all lower derivatives are zero at the edges of the compact support. That is

$$\begin{aligned} &W^{(n)}(-2h, h) = W^{(n)}(2h, h) = 0 \quad \text{for } 0 \leqslant n \leqslant \beta \\ &W^{(n)}(-2h, h) \neq 0 \text{ or } W^{(n)}(2h, h) \neq 0 \quad \text{for } n = \beta + 1 \end{aligned} \tag{4}$$

By this definition, the B-spline kernel has $\beta = 2$. In principle, $\beta \to \infty$ for the Gaussian kernel, but in practice the kernel is used in a finite domain. Consequently, the kernel and its derivatives do not decay exactly to zero within the domain. β is not well defined for a kernel with infinite support.

Aspects of the theoretical analysis presented in this paper require smoothness properties not possessed by the B-spline kernel (the significance of this restriction will be discussed). Two new polynomial kernels have been devised for this reason, and also to explore the effects of kernel function smoothness. The new kernels W_8 and W_{10} are eighth- and tenth-order polynomials with boundary smoothness of 2 and 4, respectively. They are defined by $W_n(r_a, h) = (1/h) \sum_{k=0,2,\ldots}^{n} a_k (r_a/h)^k$, where the coefficients a_k are given in Table I. They have discontinuities in third and fifth derivatives, respectively, only at the edges of the compact support. Superficially, they resemble the widely used cubic B-spline kernel. The four kernels mentioned here are plotted in Figure 1. Numerical results presented in this paper were obtained with the 10th-order polynomial, except where stated otherwise.

2.2. Assumptions

There are a few restrictions on the theoretical analysis to follow. The kernel is assumed to be compactly supported, so that $W(\mathbf{x} - \mathbf{x}_a, h)$ is zero valued for $|\mathbf{x} - \mathbf{x}_a| \geqslant 2h$. Both the kernel and the data function $A(\mathbf{x})$ are required to be infinitely differentiable within the compact support.

Copyright © 2005 John Wiley & Sons, Ltd.

Table I. Coefficients a_k of $(r_a/h)^k$ in the kernel functions W_8 and W_{10}.

n	a_0	a_2	a_4	a_6	a_8	a_{10}
8	0.603764	−0.580823	0.209206	−0.0334338	0.00200000	
10	0.676758	−0.845947	0.422974	−0.105743	0.0132179	−0.000660896

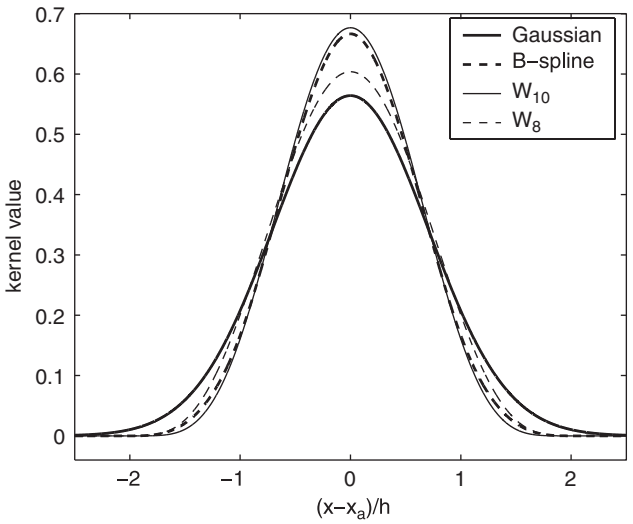

Figure 1. 1D versions of the four kernel functions used in this work. W_8 and W_{10} denote 8th- and 10th-order polynomial kernels, respectively.

Discontinuities in derivatives of $W(\mathbf{x}-\mathbf{x}_a, h)$ are allowed at the boundary of the compact support, $|\mathbf{x}-\mathbf{x}_a| = 2h$, and are described by the parameter β defined above. It is implicit throughout this paper that SPH operations on particle a are conducted with a single smoothing length h, which may be associated with that particle or may be a constant for all particles in a particular application.

Kernel functions are usually even, so that $W(\mathbf{x}-\mathbf{x}_a, h) = W(\mathbf{x}_a-\mathbf{x}, h)$, and normalized so that they satisfy $\int W(\mathbf{x}-\mathbf{x}_a, h)\,\mathrm{d}V = 1$. However, some consistency-corrected particle methods do not satisfy these criteria, so normalization and evenness are not assumed as general properties from the outset. These assumptions will be introduced for the analysis of standard SPH only.

2.3. Notation

It is useful to express the kernel in a dimensionless form, which is defined by Equation (5) for the 1D case.

$$\hat{W}_a(s) = hW(x-x_a, h), \quad s = \frac{x-x_a}{h}, \quad s_b = \frac{x_b-x_a}{h} \tag{5}$$

Copyright © 2005 John Wiley & Sons, Ltd.

Some relationships between the dimensional and non-dimensionalized forms are given in Equations (6) and (7).

$$\frac{\partial^n W(x-x_a,h)}{\partial x^n} = \frac{1}{h^{n+1}}\frac{\partial^n \hat{W}}{\partial s^n} = \frac{1}{h^{n+1}}\hat{W}^{(n)} \tag{6}$$

$$\int_{x_a-2h}^{x_a+2h} f(x)\,\mathrm{d}x = h\int_{-2}^{2} f(s)\,\mathrm{d}s \tag{7}$$

In the interests of conciseness, it is implied throughout the remainder of this paper that the particle of interest is particle a. As h is assumed to be a constant, it can be omitted from $W(x-x_a,h)$. Where there is no ambiguity, $W(x-x_a)$ and $\hat{W}(s)$ are further abbreviated to W and $\hat{W}$, respectively. Derivatives of W and $\hat{W}$ are always implicitly taken with respect to x or s, respectively, and denoted by primes or the $f^{(n)}(x)$ notation. Subscripts a and b denote the particle at which a function or derivative is to be evaluated. Similar notation will be used for the data function $A(x)$, though it will not be written in terms of s. Integrals are taken over the compact support unless otherwise stated.

3. STANDARD SPH IN ONE DIMENSION

Error in the integral or smoothing stage of the approximation has been considered by Monaghan [3] and many others, and is discussed briefly here. In the integral in Equation (1), if $A(x)$ is smooth, it can be expanded in a Taylor series about x_a. With an integration by parts, this results in

$$\begin{aligned}-\int_{x_a-2h}^{x_a+2h} A(x)\frac{\partial W(x-x_a,h)}{\partial x}\,\mathrm{d}x = {} & \left.\frac{\partial A(x)}{\partial x}\right|_{x=x_a}\int_{x_a-2h}^{x_a+2h} W(x-x_a,h)\,\mathrm{d}x \\ & + \left.\frac{\partial^2 A}{\partial x^2}\right|_{x=x_a}\int_{x_a-2h}^{x_a+2h}(x-x_a)W(x-x_a,h)\,\mathrm{d}x \\ & + \left.\frac{1}{2}\frac{\partial^3 A}{\partial x^3}\right|_{x=x_a}\int_{x_a-2h}^{x_a+2h}(x-x_a)^2 W(x-x_a,h)\,\mathrm{d}x \\ & + \cdots\end{aligned} \tag{8}$$

In terms of the non-dimensional form of the kernel, with more compact notation, the smoothing error is given by

$$-\int W'A\,\mathrm{d}x - A'_a = A'_a\left(\int \hat{W}\,\mathrm{d}s - 1\right) + hA''_a\int s\hat{W}\,\mathrm{d}s + \frac{h^2}{2}A'''_a\int s^2\hat{W}\,\mathrm{d}s + \cdots \tag{9}$$

The kernel integrals in this series depend only on the dimensionless shape of the kernel, and not on any length scales of a particular problem. For most versions of SPH, with a normalized

Copyright © 2005 John Wiley & Sons, Ltd.

and even kernel, the first two terms on the right-hand side vanish, as do all terms involving even-order derivatives. The error is then

$$-\int W'A\,\mathrm{d}x - A'_a = \frac{h^2}{2}A'''_a \int s^2 W\,\mathrm{d}s + O(h^4) \tag{10}$$

which is second-order in h. As it includes only odd derivatives of the data function $A(x)$, it is entirely dispersive and free of dissipation.

This is the contribution to error due to the smoothing stage, and is independent of particle distribution. Discretization error and resultant overall error are considered in Sections 3.1 and 3.2 for standard SPH with uniform and arbitrary particle distribution, respectively. Each treatment consists of a theoretical analysis followed by a presentation of quantitative results of both analysis and numerical experiments.

3.1. Uniform particle spacing

3.1.1. Analysis. Discretization error is the error introduced when the smoothing integral in Equation (1) is approximated with a discrete version based on data and kernel values at particles. Each particle b is located at x_b and associated with a volume (length in 1D) Δx_b. Here it is assumed that the volumes span the compact support without gaps or overlaps. In the special case when particles are evenly spaced, $\Delta x_b = \Delta x$ for all b. The approximate SPH integral can be described usefully by the second Euler–MacLaurin formula [29]. For a general function $f(x)$, this is

$$\Delta x \sum_{j=1}^{n} f_j = \int_{x_1-\Delta x/2}^{x_n+\Delta x/2} f(x)\,\mathrm{d}x + \sum_{k=1}^{\infty} \frac{B_{2k}\Delta x^{2k}}{(2k)!}(1-2^{-2k+1})(f_{(n+1/2)}^{(2k-1)} - f_{1/2}^{(2k-1)}) \tag{11}$$

where f_j is defined as $f(x_1 + j\Delta x)$ and $f(x)$ is smooth. B_{2k} are the Bernoulli numbers, which increase non-monotonically with k, but not as rapidly as $(2k)!$ in the denominator. If $f(x)$ is defined as $A(x)W'(x)$ for the present problem, the left-hand side of Equation (11) is identical to the SPH estimate of $A'(x_a)$, the first term on the right-hand side represents its integral counterpart, and the remainder is an exact expression for the discretization error. $f_{n+1/2}^{(2k-1)}$ and $f_{1/2}^{(2k-1)}$ are the $(2k-1)$th derivatives of $A(x)W'(x)$, evaluated at the edges of the compact support.

For typical kernels, some low-order derivatives are zero at the compact support boundary. This property of the kernel is described by the boundary smoothness defined above. If the boundary smoothness of the kernel W is β, the boundary smoothness of the function $A(x)W'(x)$ is $\beta-1$, and the term $f_{n+1/2}^{(2k-1)} - f_{1/2}^{(2k-1)}$ in the Euler–MacLaurin formula is zero for all $2k-1 \leqslant \beta-1$. The first non-zero term in the series has $2k = \beta+2$, assuming that β is even (the modification for odd β is straightforward). With these substitutions in Equation (11), discretization error is

$$\sum A_b W'_b \Delta x - \int AW'\,\mathrm{d}x$$

$$= \Delta x^{\beta+2}\frac{B_{\beta+2}}{(\beta+2)!}(1-2^{-\beta-1})[(AW')^{(\beta+1)}_{x=x_a+2h} - (AW')^{(\beta+1)}_{x=x_a-2h}] + O(\Delta x^{\beta+4}) \tag{12}$$

Copyright © 2005 John Wiley & Sons, Ltd.

$A(x)$ in the error term is now expanded in a Taylor series about x_a, and the kernel is written in the non-dimensional form to make its dependence on smoothing length explicit. Derivatives of AW' are then expressed as follows:

$$(AW')^{(\beta+1)} = \frac{A_a}{h^{\beta+3}}\,\hat{W}^{(\beta+2)} + \frac{A'_a}{h^{\beta+2}}[s\hat{W}^{(\beta+2)} + (\beta+1)\hat{W}^{(\beta+1)}] + \frac{A''_a}{2h^{\beta+1}}[s^2\hat{W}^{(\beta+2)} + 2s(\beta+1)\hat{W}^{(\beta+1)} + (\beta+1)\beta\hat{W}^{(\beta)}] + O\left(\frac{1}{h^{\beta}}\right) \tag{13}$$

This representation is now substituted into the term in square brackets in Equation (13) and evaluated at $x = x_a \pm 2h$. If the kernel is even, even-order derivatives of $A(x)$ cancel to give

$$\begin{aligned}[(AW')^{(\beta+1)}_{x=x_a+2h} - (AW')^{(\beta+1)}_{x=x_a-2h}] &= \frac{A'_a}{h^{\beta+2}}[4\hat{W}^{(\beta+2)}_{s=2} + 2(\beta+1)\hat{W}^{(\beta+1)}_{s=2}] \\ &+ \frac{A'''_a}{3h^{\beta}}[8\hat{W}^{(\beta+2)}_{s=2} + 12(\beta+1)\hat{W}^{(\beta+1)}_{s=2} + 6(\beta+1)\beta\hat{W}^{(\beta)}_{s=2} + (\beta+1)\beta(\beta-1)\hat{W}^{(\beta-1)}_{s=2}] \\ &+ O\left(\frac{1}{h^{\beta-2}}\right)\end{aligned} \tag{14}$$

Substitution of this expression into Equation (13) leads to this final statement of discretization error

$$\sum A_b W'_b \Delta x - \int AW'\,\mathrm{d}x = \left(\frac{\Delta x}{h}\right)^{\beta+2} \frac{B_{\beta+2}}{(\beta+2)!}(1-2^{-\beta-1}) \times \{A'_a[4\hat{W}^{(\beta+2)}_{s=2} + 2(\beta+1)\hat{W}^{(\beta+1)}_{s=2}] + O(h^2)\} + O\left(\left[\frac{\Delta x}{h}\right]^{\beta+4}\right) \tag{15}$$

This can be combined with Equation (10) for smoothing error to obtain the following expression for overall error:

$$\begin{aligned}-\sum A_b W'_b \Delta x - A'_a &= +\frac{h^2}{2}A'''_a \int s^2\hat{W}\,\mathrm{d}s + O(h^4) - \left(\frac{\Delta x}{h}\right)^{\beta+2} \frac{B_{\beta+2}}{(\beta+2)!}(1-2^{-\beta-1}) \\ &\times \{A'_a[4\hat{W}^{(\beta+2)}_{s=2} + 2(\beta+1)\hat{W}^{(\beta+1)}_{s=2}] + O(h^2)\} + O\left(\left[\frac{\Delta x}{h}\right]^{\beta+4}\right)\end{aligned} \tag{16}$$

This is an exact expression for error in the SPH gradient approximation at a particle a, in terms of the data function and its derivatives at x_a, the smoothing length, the particle spacing

Copyright © 2005 John Wiley & Sons, Ltd.

and the kernel function. It is valid for uniformly spaced particles in one dimension, smooth data functions, and kernel functions which are smooth (except at the support boundary), even and normalized. It also requires that the particle volumes span the compact support without gaps or overlaps.

It is clear that the total error is the sum of a second-order error in h (smoothing error) and an order $(\beta+2)$ error in $\Delta x/h$ (due to discretization of the smoothing integral). The coefficient of $(\Delta x/h)^{\beta+2}$ in the discretization error contains terms of second order in h, as well as terms which are independent of h. Therefore, as $(\Delta x/h)$ is reduced, accuracy becomes limited by smoothing error of order h^2. This is to be expected, as the SPH approximation approaches the continuous smoothing defined by the integration stage of Equation (1). On the other hand, as smoothing length h tends to zero, error does not vanish, but becomes dominated by a residual term which depends on $(\Delta x/h)$. The kernel boundary smoothness, β, determines the behaviour of this error term.

3.1.2. Quantitative results. Error predicted by the theoretical analysis has been calculated for various particle distributions and a chosen data function, and the results are presented here in a series of graphs. In all cases the data function was the sinusoid $A(x)=A_0\sin(2\pi x/\lambda)$. The wavelength λ can be considered representative of a wavelength of interest in a real application. Equation (16) was evaluated for this choice of $A(x)$ with additional terms up to the first two non-zero terms of the Euler–MacLaurin summation and the first two terms of the Taylor series of $A(x)$, i.e. the A'_a and A'''_a terms shown in full in Equation (14). The smoothing error series of Equation (9) was also evaluated to the first two non-zero terms, which involve $h^2A'''_a$ and $h^4A^{(5)}_a$. The analysis requires that the volumes Δx of a particle's neighbours fill that particle's kernel support of width $4h$, without gaps or overlaps. Therefore, as there is always a particle at the centre of the compact support, the analysis can be expected to be exact for particle distributions satisfying

$$\frac{\Delta x}{h}=\frac{4}{2n+1} \tag{17}$$

where n is an integer. The analytically predicted error according to Equation (16) has been quantified only for these conditions and is plotted with discrete points and labelled 'analytical' in the graphs below.

Numerical experiments have also been conducted, both to validate the theoretical analysis and to aid overall insight. The SPH estimate of the data function's first derivative was compared with the exact derivative to determine the error empirically. For both the analytical and empirical calculations, error was computed at all particles over an interval of one wavelength λ, and results are presented in the form of non-dimensionalized L_2 norm error. The dimensionless error is the ratio of the computed error to the maximum absolute value of the exact derivative of the data function, which is $2\pi A_0/\lambda$. Empirically computed error is plotted as continuous curves made up 50–200 data points each, labelled 'empirical' in the graph legends. The combinations of h and $\Delta x/h$ chosen for empirical evaluation are not limited to those satisfying Equation (17), and include many intermediate values.

Results are presented in Figure 2(a) as functions of h/λ (the ratio of smoothing length to wavelength) and in Figure 2(b) as functions of $\Delta x/h$ (the ratio of particle spacing to smoothing length). For particle distributions satisfying Equation (17), Figure 2 displays close agreement between the error analysis and empirically computed error. Figure 2(a) confirms that error is

Copyright © 2005 John Wiley & Sons, Ltd.

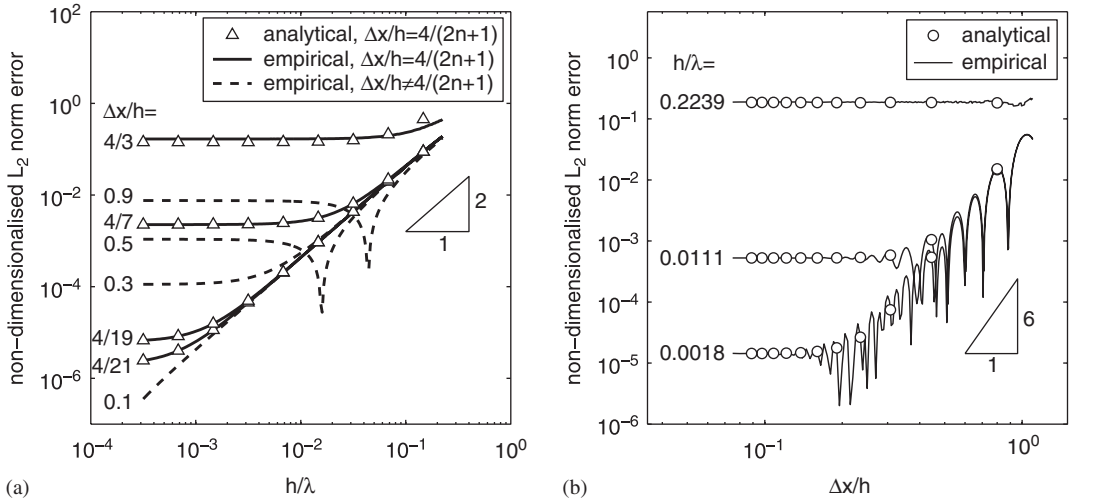

Figure 2. Analytically and empirically calculated L_2 norm of error in SPH estimates of the first derivative of $A(x) = A_0 \sin(2\pi x/\lambda)$: (a) as a function of smoothing length for various values of particle spacing; and (b) as a function of particle spacing for various smoothing lengths.

second-order in smoothing length, but is limited at low h by discretization error. For particle distributions that do not satisfy $\Delta x/h = 4/(2n+1)$, there is a special h/λ value at which error is zero (but because the empirical curves are based on a finite number of points, and the scales are logarithmic, these error minima appear greater than zero in Figure 2).

The variation of error with $\Delta x/h$ is not monotonic. Closer investigation has shown that the numerous local minima in Figure 2(b) again correspond to points where the error changes sign. For the discrete $\Delta x/h$ values satisfying $\Delta x/h = 4/(2n+1)$ (i.e. the particle distributions for which the theoretical analysis should be exact), error displays order $(\Delta x/h)^{(\beta+2)}$ behaviour, with $\beta = 4$ for the 10th-order polynomial kernel used here.

A comparison of empirically evaluated error for various kernel functions is presented in Figure 3(a). A low value of smoothing length has been selected here for illustrative purposes, so that error is dominated by discretization effects. The predictions of the analysis for discretization-limited error are borne out—error for the 8th-order polynomial kernel ($\beta = 2$) decays less rapidly than error observed with the 10th-order polynomial kernel ($\beta = 4$). The Gaussian kernel displays higher order discretization error behaviour. Smoothing-limited error (that is, total error at low $\Delta x/h$) is greater for the Gaussian kernel than for the others. This is due to the integral moments in the smoothing error series of Equation (9), which are higher for the Gaussian kernel than for the others tested. In Figure 3(b), it is apparent that errors with the B-spline and 8th-order polynomial kernels display similar dependence on $\Delta x/h$. This is predicted by the analysis, since $\beta = 2$ for both kernels. These plots also demonstrate that the qualitative predictions of the discretization error model appear to be valid for the B-spline kernel, despite the fact that it is not infinitely smooth inside the compact support. Smoother kernels appear to give more rapid convergence to the smoothing-limited regime as $\Delta x/h$ is reduced.

Copyright © 2005 John Wiley & Sons, Ltd.

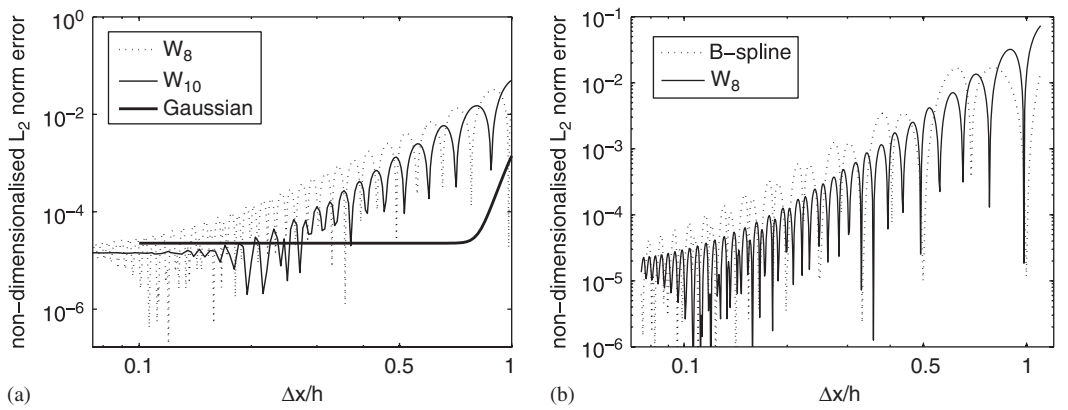

Figure 3. Observed rms error in SPH estimates of the first derivative of $A(x) = A_0 \sin(2\pi x/\lambda)$ for: (a) 8th-order polynomial, 10th-order polynomial and Gaussian kernels; and (b) the B-spline and 8th-order polynomial kernels. $h/\lambda = 0.0018$ in all cases.

3.2. Arbitrary particle spacing

3.2.1. Analysis. To examine the effects of non-uniform particle distribution, the smoothing approximation integral $\int AW'\,\mathrm{d}x$ can be partitioned into a series of integrals over subintervals, each of which represents the volume of a particle. Each of these volumes has width of Δx_b and is centred at a location $\bar{x}_b$ which does not necessarily coincide with the particle location, x_b. These integrals over particle volumes are reformulated by expanding $A(x)$ about x_a and $W(x)$ about x_b. The assumption of an even, normalized kernel is retained. The procedure is as follows:

$$-\int_{x_a-2h}^{x_a+2h} AW'\,\mathrm{d}x = -\sum_b \int_{\bar{x}_b-\Delta x_b/2}^{\bar{x}_b+\Delta x_b/2} AW'\,\mathrm{d}x$$

$$= -\sum_b \int_{\bar{x}_b-\Delta x_b/2}^{\bar{x}_b+\Delta x_b/2} [A_a+(x-x_a)A'_a+\cdots][W'_b+(x-x_b)W''_b+\cdots]\,\mathrm{d}x \qquad (18)$$

The product within the integral is now expanded, and A_a in the resulting term $A_a W'_b$ is replaced with A_b by means of another Taylor series to give

$$-\int_{x_a-2h}^{x_a+2h} AW'\,\mathrm{d}x = -\sum_b A_b W'_b \Delta x - \sum_b \left(A'_a \hat{W}'_b + \frac{1}{h} A_a \hat{W}''_b\right) \int (s-s_b)\,\mathrm{d}s$$

$$-\sum_b \frac{1}{2h} A_a \hat{W}'''_b \int (s-s_b)^2\,\mathrm{d}s - \sum_b A'_a \hat{W}''_b \int s(s-s_b)\,\mathrm{d}s$$

$$-\sum_b \frac{h}{2} A''_a \hat{W}'_b \left(\int s^2\,\mathrm{d}s - s_b^2 \int \mathrm{d}s\right) + \cdots \qquad (19)$$

This equation is expressed in dimensionless form, and all integrals on the right-hand side are taken from $\bar{x}_b - \Delta x_b/2$ to $\bar{x}_b + \Delta x_b/2$. Δs_b and $\bar{s}_b$ are now introduced to denote the

Copyright © 2005 John Wiley & Sons, Ltd.

dimensionless subinterval width $\Delta x_b/h$ and centroid location $(\bar{x}_b - x_a)/h$, respectively. The parameter $\delta_b = (\bar{x}_b - x_b)/\Delta x_b$ is used as a dimensionless measure of particle distribution non-uniformity. Equation (20) results as a general expression for discretization error.

$$-\sum_b A_b W'_b \Delta x + \int_{x_a-2h}^{x_a+2h} A W' \,\mathrm{d}x = A'_a \sum_b \hat{W}'_b \delta_b \Delta s_b^2 + \frac{A_a}{h} \sum_b \hat{W}''_b \delta_b \Delta s_b^2$$
$$+ \frac{A_a}{2h} \sum_b \hat{W}'''_b \left(\frac{\Delta s_b^2}{12} + \delta_b^2 \Delta s_b^2 \right) \Delta s_b + A'_a \sum_b \hat{W}''_b \left(\frac{\Delta s_b^2}{12} + \bar{s}_b \delta_b \Delta s_b \right) \Delta s_b$$
$$+ A''_a \frac{h}{2} \sum_b \hat{W}'_b \left(\frac{\Delta s_b^2}{12} + (\bar{s}_b + s_b) \delta_b \Delta s_b \right) \Delta s_b + O(h^2) \tag{20}$$

To gain some insight into the nature of this error, the terms Δs_b and δ_b are now replaced by average values Δs and δ and moved outside the summations (introducing a higher order error into the analysis itself). One Δs_b is retained inside each sum, resulting in sums such as $\sum \hat{W}'_b \Delta s_b$, which can be interpreted as an approximation to $\int \hat{W}' \,\mathrm{d}s$. Because of the assumed evenness of the kernel function, most of the integrals approximated by summations in Equation (20) evaluate exactly to zero. The only exception is the following component of the last sum:

$$A''_a \frac{h}{2} \Delta s \delta \sum_b \hat{W}'_b (\bar{s}_b + s_b) \Delta s_b \approx A''_a \frac{h}{2} \Delta s \delta \int 2s \hat{W}' \,\mathrm{d}s = -A''_a h \Delta s \delta \int \hat{W} \,\mathrm{d}s = A''_a h \Delta s \delta O(1) \tag{21}$$

The approximate integrals are similar to the weighted Monte Carlo integrals studied by Yakowitz *et al.* [30], which have errors of order Δs_b^2. The first four sums on the right-hand side of Equation (20), approximating integrals which evaluate to zero, are therefore replaced with an $O(\Delta s)^2$ term. The integral represented by the last sum does not equal zero; it is substituted by Equation (21), with an additional $O(\Delta s)^2$ error. This yields a final expression for discretization error for arbitrarily spaced particles with normalized even kernel functions:

$$-\sum_b A_b W'_b \Delta x + \int_{x_a-2h}^{x_a+2h} A W' \,\mathrm{d}x$$
$$= \frac{A_a}{h} \left[\delta O(\Delta s^3) + \frac{1}{2} \left(\delta^2 + \frac{1}{12} \right) O(\Delta s^4) \right] + A'_a [\delta O(\Delta s^3) + O(\Delta s^4)]$$
$$\times A''_a h [\delta O(\Delta s) + \delta O(\Delta s^3) + O(\Delta s^4)] + \cdots \tag{22}$$

Combining this with Equation (10), and neglecting some lower order terms, results in the following expression for overall error:

$$-\sum_b A_b W'_b \Delta x - A'_a = \frac{A_a}{h} \left[\delta O(\Delta s^3) + \frac{1}{2} \left(\delta^2 + \frac{1}{12} \right) O(\Delta s^4) \right] + A'_a [\delta O(\Delta s^3) + O(\Delta s^4)]$$
$$\times A''_a h [\delta O(\Delta s) + O(\Delta s^4)] + \cdots + \frac{h^2}{2} A'''_a \int s^2 \hat{W} \,\mathrm{d}s + \cdots \tag{23}$$

Copyright © 2005 John Wiley & Sons, Ltd.

Equation (23) is an expression of the interaction between the three parameters h, $\Delta x/h$ ($=\Delta s$) and δ. Although it does not allow exact quantification of error like Equation (16), it provides important insights. The leading terms are first-order in $\Delta x/h$, first-order in the non-uniformity parameter δ, and order $1/h$ in smoothing length. These properties are independent of the smoothness of the kernel. The most striking feature of Equation (23) is the $1/h$ term, which suggests that discretization error will ultimately increase if h is decreased while $\Delta x/h$ and δ are held constant.

3.2.2. Quantitative results. In numerical experiments, non-uniform spacing was introduced by adding a normally distributed random perturbation to the position of every particle in the numerical experiment. The normalized standard deviation of this perturbation, $\sigma/\Delta x$, is an empirical measure of the parameter $\delta_b = (\bar{x}_b - x_b)/\Delta x_b$, though its meaning is not exactly the same. The analytical statement of error, Equation (23), has not been evaluated numerically, as it contains many order-of-magnitude terms.

The empirical results shown in Figure 4 confirm the theoretical finding that error is second-order in h when h is relatively large (as with uniform spacing), but error is of order h^{-1} when h is sufficiently small. The data in Figure 5(a) (for a small h/λ value of 0.022) suggest that discretization error is third-order in $\Delta x/h$. This is consistent with the $(1/h)O(\Delta x^3/h^3)$ term in the theoretical analysis, which may dominate under conditions of sufficiently small h and large $\Delta x/h$. The upper envelope on the curves for the uniform and least non-uniform particle distributions ($\sigma/\Delta x = 0$ and $\sigma/\Delta x = 0.002$) is steeper, suggesting that discretization error is dominated by the $O(\Delta x^4/h^4)$ term in Equation (23) when non-uniformity is small. Results for larger smoothing length are shown in Figure 5(b). Error is independent of $\Delta x/h$ for most of the range tested, showing that the smoothing error dominates. Error is first-order in $\Delta x/h$ for distributions with severe non-uniformity and high values of $\Delta x/h$, suggesting that the $h\delta O(\Delta s)$ term of Equation (23) is dominant in this regime.

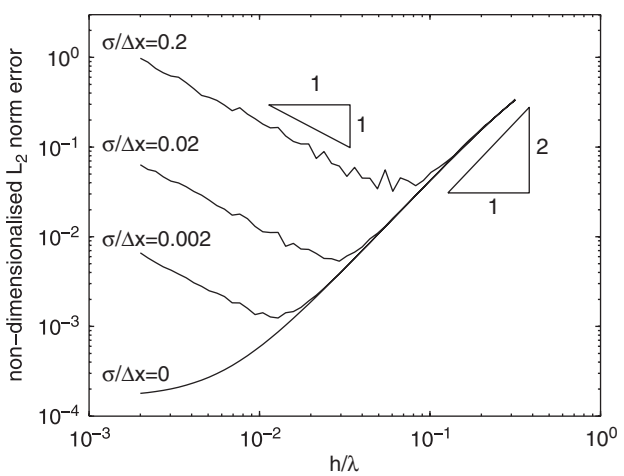

Figure 4. Observed L_2 norm error in SPH estimates of the first derivative of $A(x) = A_0 \sin(2\pi x/\lambda)$ as a function of smoothing length, for various particle spacing perturbations, computed with $\Delta x/h = 0.364$.

Copyright © 2005 John Wiley & Sons, Ltd.

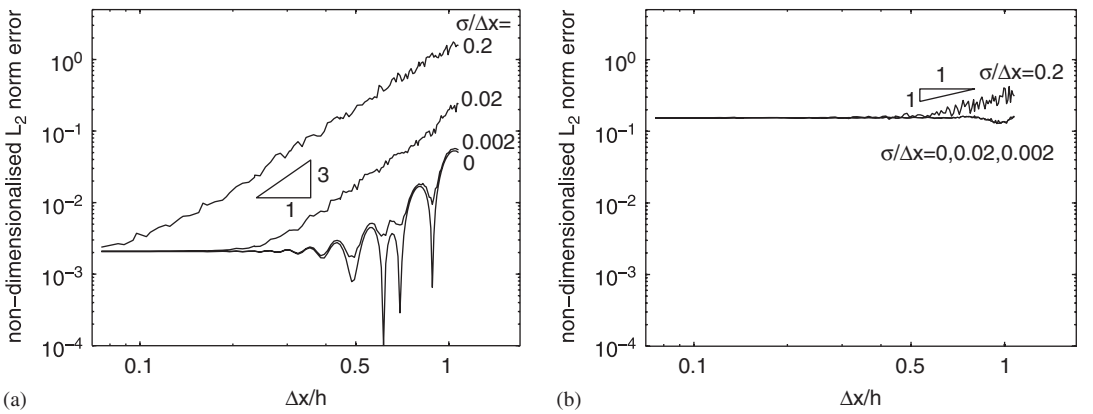

Figure 5. Observed L_2 norm error in SPH estimates of the first derivative of $A(x) = A_0 \sin(2\pi x/\lambda)$ as a function of particle spacing for various particle spacing perturbations with: (a) $h/\lambda = 0.022$; and (b) $h/\lambda = 0.2$.

4. FIRST-ORDER CONSISTENT METHODS IN ONE DIMENSION

Various particle methods have been proposed to remedy the lack of consistency in SPH. An nth-order consistent method is one which exactly evaluates values and derivatives of polynomial data functions up to order n, for arbitrary particle distributions. Here we consider the error properties of a general first-order consistent method.

4.1. Analysis

The total error in the first derivative has been analyzed above for arbitrary particle distribution and an even, normalized kernel function, resulting in Equation (23). However, kernel functions developed through consistency correction techniques are neither normalized nor even, in general. Equation (9) for smoothing error can be combined with Equation (20) for discretization error to obtain the following more general expression which is valid for non-even, non-normalized kernels:

$$
\begin{aligned}
&-\sum_b A_b W'_b \Delta x - A'_a \\
&\quad = A'_a \left(\int \hat{W}\, \mathrm{d}s - 1 \right) + h A''_a \int s \hat{W}\, \mathrm{d}s + \frac{h^2}{2} A'''_a \int s^2 \hat{W}\, \mathrm{d}s + \cdots \\
&\qquad + A'_a \sum_b \hat{W}'_b \delta_b \Delta s_b^2 + \frac{A_a}{h} \sum_b \hat{W}''_b \delta_b \Delta s_b^2 + \frac{A_a}{2h} \sum_b \hat{W}'''_b \left(\frac{\Delta s_b^2}{12} + \delta_b^2 \Delta s_b^2 \right) \Delta s_b \\
&\qquad + A'_a \sum_b \hat{W}''_b \left(\frac{\Delta s_b^2}{12} + \bar{s}_b \delta_b \Delta s_b \right) \Delta s_b + A''_a \frac{h}{2} \sum_b \hat{W}'_b \left(\frac{\Delta s_b^2}{12} + (\bar{s}_b + s_b) \delta_b \Delta s_b \right) \Delta s_b \\
&\qquad + O(h^2)
\end{aligned}
\tag{24}
$$

Copyright © 2005 John Wiley & Sons, Ltd.

If the method is first-order consistent, then all error series terms in $A(x)$ and $A'(x)$ must vanish. Eliminating these terms from Equation (24), the error for a first-order consistent method is

$$-\sum_b A_b W'_b \Delta x - A'_a = hA''_a \int s\hat{W}\,\mathrm{d}s + \frac{h^2}{2}A'''_a \int s^2 \hat{W}\,\mathrm{d}s + \cdots + A''_a \frac{h}{2}\sum_b \hat{W}'_b \left(\frac{\Delta s_b^2}{12} + (\bar{s}_b + s_b)\delta_b \Delta s_b\right)\Delta s_b + O(h^2) \tag{25}$$

In comparison with Equation (23) for standard SPH, consistency correction has eliminated the $1/h$ discretization error, which caused divergence for non-uniform particle distributions. The normalization error ($\int \hat{W}\,\mathrm{d}s - 1$) is not zero, but it is a contributor to the coefficient of A'_a, which must vanish by virtue of the consistency property. However, non-evenness of the corrected kernel results in a first-order smoothing error term $hA''_a \int s\hat{W}\,\mathrm{d}s$. It should be noted that asymmetry in the corrected kernel is due to non-uniformity and asymmetry of the particle distribution. The significance of the new first-order smoothing error (the first term on the right-hand side of Equation (26)) can be expected to increase with increasingly non-uniform particle distributions. Discretization error is dominated by another $O(1/h)$ term. It is difficult to interpret Equation (26) further because the corrected kernel function depends implicitly on the particle distribution and hence on Δx and δ.

4.2. Implementations

Two of the many first-order consistent developments of SPH are outlined here. Results of numerical experiments are presented here for one of the two methods in one dimension, and results for both methods will be presented in 3D.

In the first-order form of RKPM, due to Liu *et al.* [19], a basic kernel or window function $W(\mathbf{x} - \mathbf{x}_a)$ is multiplied by a polynomial $\mathbf{cP}(\mathbf{x} - \mathbf{x}_a)$, where $\mathbf{P}(\mathbf{x}) = (1, x, y, z)^{\mathrm{T}}$ and $\mathbf{c}$ is the vector of coefficients, determined by solving

$$\left[\sum_b W(\mathbf{x}_b - \mathbf{x})\mathbf{P}(\mathbf{x}_b)\mathbf{P}(\mathbf{x}_b - \mathbf{x})^{\mathrm{T}}\right]\mathbf{c}(\mathbf{x})^{\mathrm{T}} = \mathbf{P}(\mathbf{x}) \tag{26}$$

This equation guarantees that linear functions are exactly reproduced. In order to determine derivatives of the overall kernel function $W(\mathbf{x})\mathbf{cP}(\mathbf{x})$, Equation (26) can be differentiated to obtain an implicit expression for derivatives of $\mathbf{c}$. Particle volumes, which weight the individual particle contributions in SPH, are set to unity in RKPM.

Another method to ensure first-order consistency is the mixed kernel and gradient correction proposed by Bonet and Lok [21]. A zero-order consistent corrected kernel function is defined by

$$\tilde{W}(\mathbf{x}_b - \mathbf{x}) = \frac{W(\mathbf{x}_b - \mathbf{x})}{\sum_b W(\mathbf{x}_b - \mathbf{x})V_b} \tag{27}$$

The corrected gradient $\tilde{\nabla}\tilde{W}$ is then defined as $\mathbf{L}\nabla\tilde{W}$ where the matrix $\mathbf{L}$ is defined as

$$\mathbf{L}(\mathbf{x}) = \left(\sum_b \mathbf{x}_b^{\mathrm{T}} \nabla\tilde{W}(\mathbf{x}_b - \mathbf{x})V_b\right)^{-1} \tag{28}$$

Copyright © 2005 John Wiley & Sons, Ltd.

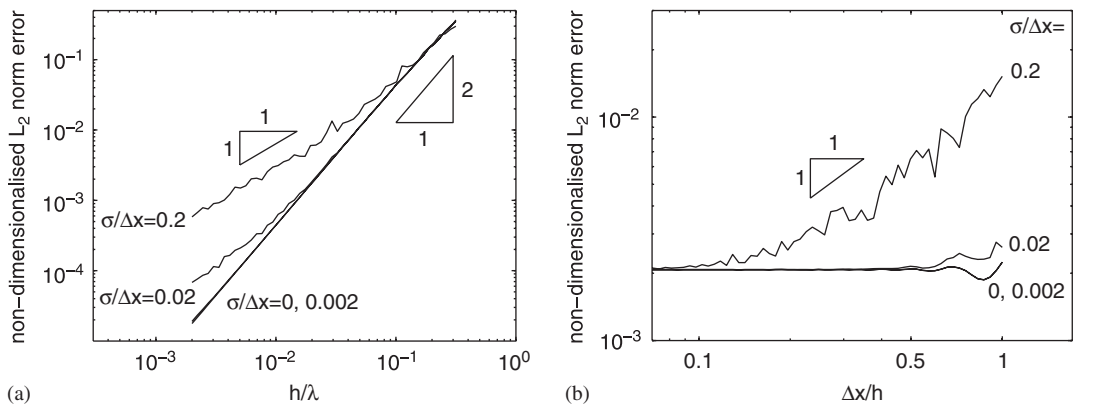

Figure 6. Empirically observed error in first-order consistent SPH gradient estimates of a sinusoidal data function for various particle spacing perturbations: (a) as a function of smoothing length h with $\Delta x/h = 0.7$; and (b) as a function of particle spacing ratio $\Delta x/h$ with $h/\lambda = 0.022$.

When determining $\nabla\tilde{W}$, it must be noted that the denominator in Equation (27) is a function of $\mathbf{x}$.

4.3. Quantitative results

In numerical experiments, error was evaluated for the first-order consistent SPH gradient correction due to Bonet and Lok [21], summarized in Equations (27) and (28). The results shown in Figure 6(a) confirm that error is first-order in smoothing length, as smoothing length tends to zero. However, for higher values of smoothing length, accuracy is second-order. The transition from second- to first-order accuracy occurs at lower smoothing lengths when the spacing is more uniform. Like standard SPH, the corrected method becomes more susceptible to the effects of non-uniform spacing as the average $\Delta x/h$ is increased.

The influence of particle spacing on the corrected method is illustrated in Figure 6(b), for which a very fine smoothing length was selected in order to highlight discretization error. Even so, particle distribution effects are significant only for the highest value of $\sigma/\Delta x$ shown. In this case, error is approximately first-order in $\Delta x/h$. This is consistent with Equation (26). These results show that enforcement of linear consistency in a SPH-like method greatly improves its robustness in the presence of non-uniform particle spacing. Despite the appearance of a new first-order smoothing error term, it appears that this error is not significant for uniform or moderately non-uniform particle spacing.

5. THREE DIMENSIONS

The full analysis of one-dimensional discrete methods does not generalize to higher dimensions because it is not clear how the compact support can be partitioned into analytically convenient subvolumes assigned to each particle. However, a brief analysis for three dimensions will be presented for error due to the continuous integral stage, and numerical experiments will be described. The analysis can easily be reduced to the two-dimensional case.

Copyright © 2005 John Wiley & Sons, Ltd.

5.1. Analysis

In the following, V is the three-dimensional compact support. $A_{x,a}$ denotes a partial derivative evaluated at particle a, and integrals are taken over V unless otherwise indicated. s_i are the dimensionless co-ordinates x/h, etc. and $\hat{V}$ is the non-dimensionalized volume V/h^3. All integrals are volume integrals over the kernel support. For convenience, the co-ordinate system has its origin at a, the particle of interest.

The continuous SPH approximation to $\partial A/\partial x$ is $-\int_V W A_x \, \mathrm{d}V$. With integration by parts, a Taylor series expansion and non-dimensionalization, the error in this approximation is

$$-\int_V A \frac{\partial W}{\partial x_i} \mathrm{d}V - \left.\frac{\partial A}{\partial x_i}\right|_a = \left.\frac{\partial A}{\partial x_i}\right|_a \left(\int \hat{W} \, \mathrm{d}\hat{V} - 1\right) + h \left(\left.\frac{\partial^2 A}{\partial x_i x_j}\right|_a \int s_j \hat{W} \, \mathrm{d}\hat{V}\right) + \frac{h^2}{2} \left(\left.\frac{\partial^3 A}{\partial x_i x_j x_k}\right|_a \int s_j s_k \hat{W} \, \mathrm{d}\hat{V}\right) + O(h^3) \tag{29}$$

where summation over repeated indices i, j and k is implied.

This is a multidimensional equivalent of Equation (9), and the structure of the error series is essentially the same as in one dimension. If the kernel is normalized ($\int \hat{W} \, \mathrm{d}\hat{V} = 1$) and symmetric about all three axes, the first two terms on the right-hand side disappear and smoothing error is second-order. As in the 1D case, asymmetric consistency-corrected kernels will result in a first-order smoothing error term.

5.2. Numerical experiments

Three-dimensional numerical experiments were conducted with the sinusoidal test data function $A(\mathbf{x}) = A_0 \sin(2\pi \mathbf{x} \cdot \mathbf{n}/\lambda)$. The magnitude of the vector error in ∇A was evaluated at every point in a sphere of diameter equal to λ, and the L_2 norm of this error was calculated and non-dimensionalized. Enough particles were placed outside the sphere to eliminate boundary effects. Particles were distributed on a regular Cartesian grid, and randomized when desired with a normally distributed perturbation. Tests were conducted with the unit vector $\mathbf{n}$ aligned with the x-axis, and also with $\mathbf{n} = (\sqrt{3/5}, \sqrt{1/5}, \sqrt{1/5})$. The 3D tests differ from the 1D tests in that particle volumes were calculated by a method used in SPH physics simulations. Density was calculated as $\rho_a = \sum_b W_{ab} m$, where every particle has equal mass m, and volume was then determined from $V_b = m/\rho_b$. In this regard, the three-dimensional test is more realistic than the one-dimensional test.

Results are shown in Figure 7. The trends predicted analytically and observed empirically in one dimension appear to be reproduced in three dimensions. With uniformly spaced particles, error decays with h^2 for high h, and is discretization-limited at low h. This is somewhat surprising; the significance of uniform distribution in the 1D analysis is that particles are located at the centroids of assigned subvolumes which fill the compact support exactly, without gaps or overlaps. It is not obvious that this criterion can be satisfied for a Cartesian distribution of particles with a spherically symmetric 3D kernel. Comparison of Figure 7(a) with Figure 7(b) shows that error is not sensitive to the orientation of the data gradient with respect to the particle distribution.

Copyright © 2005 John Wiley & Sons, Ltd.

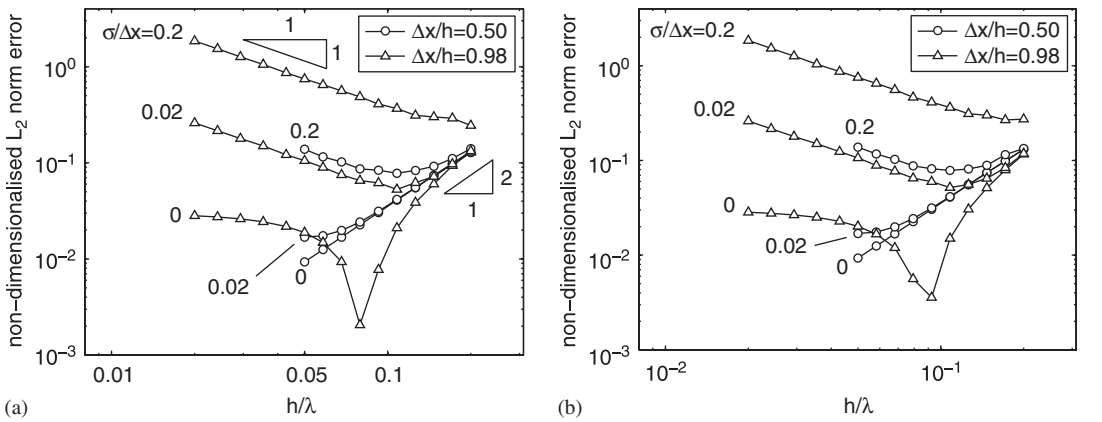

Figure 7. Empirically observed error in 3D SPH gradient estimates of a sinusoidal data function for various values of mean particle spacing $\Delta x/h$ and spacing perturbation $\sigma/\Delta x$: (a) the data gradient is aligned with the baseline unperturbed particle distribution; and (b) it is oblique.

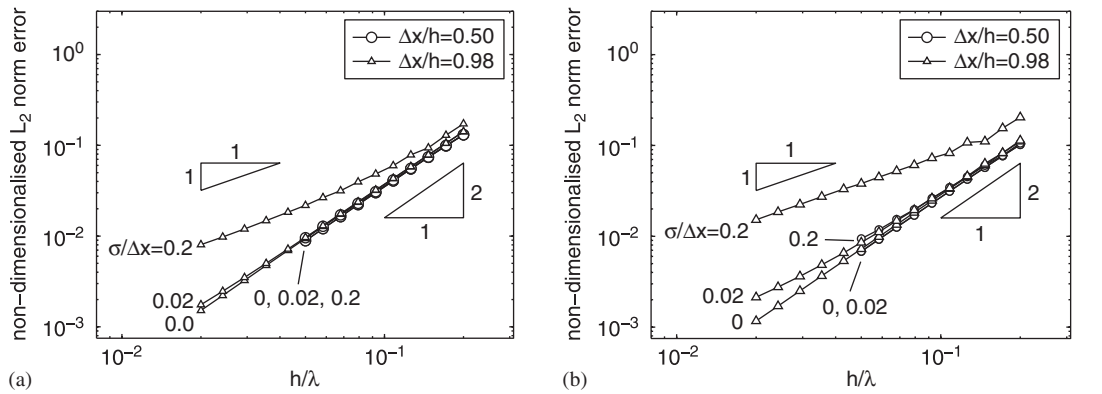

Figure 8. Observed L_2 norm error in 3D in estimates of the gradient of $A(\mathbf{x}) = A_0 \sin(2\pi \mathbf{x} \cdot \mathbf{n}/\lambda)$, for various values of mean particle spacing $\Delta x/h$ and spacing perturbation $\sigma/\Delta x$ with: (a) first-order consistent gradient-corrected SPH; and (b) first-order consistent RKPM.

Finally, results are shown in Figure 8 for two first-order consistent methods applied to uniformly and non-uniformly spaced particles. The one-dimensional result is reproduced in 3D: for low smoothing length, the divergent behaviour of standard SPH is replaced with first-order discretization-limited error. The results of gradient correction and RKPM are similar, but the gradient correction method displays slightly less sensitivity to non-uniform particle spacing.

Han and Meng [26] have shown order $(p+1)$ convergence for p-order consistency, both theoretically and empirically, suggesting that error should be second-order in the present case of first-order consistent RKPM. However, their analysis was restricted to certain classes of particle distribution. The appearance of first-order behaviour in the present work is due to unusually large values of $\Delta x/h$ and $\sigma/\Delta x$ which have been selected in order to observe errors in extreme cases. Such poor discretizations would be avoided in practice when possible; however, the user

Copyright © 2005 John Wiley & Sons, Ltd.

can choose only the initial particle distribution, and high values of $\sigma/\Delta x$ may arise through motion of the particles.

6. CONVERGENCE OF PARTICLE GRADIENT APPROXIMATIONS

There are two length scales which affect the accuracy of SPH-like methods. These are the smoothing length h, which characterizes the radius of interaction between particles, and the ratio $\Delta x/h$, which in 1D is inversely proportional to the number of particles in the compact support. $\Delta x/h$ can also be viewed as a measure of particle overlap. Smoothing length is analogous to the element size in a mesh-based method. Intuitively, the inverse of $\Delta x/h$ is analagous to the number of nodes in the stencil of a finite difference or finite volume method, or the number and connectivity of nodes in each element in the finite element method. To preserve this analogy, it was chosen to present results in terms of h and $\Delta x/h$ in this paper, although the choice of h and Δx would have been equally valid. The analogy is useful at an intuitive level, but it is not rigorous.

For users of a mesh-based computational method, element size is the main parameter which can be used to control accuracy. Convergence means that the numerical solution approaches the exact solution as this one parameter tends to zero, and the computational stencil is considered a fixed characteristic of the method. In particle methods, for the sake of simplicity as well as the experience earned in mesh-based methods, it is desirable to vary h alone to find an acceptable trade-off of accuracy and computational cost, while holding $\Delta x/h$ constant at some suitable value (not tampering with the continuously adjustable 'stencil'). This philosophy is ingrained in much of the literature on particle methods, including this paper. However, the analysis and numerical experiments presented here show that in standard SPH, decreasing h with constant $\Delta x/h$ results in discretization-limited error at best; when spacing is non-uniform (which is inevitable in practice), it may result in divergence. Second-order convergence is observed at sufficiently large h and small $\Delta x/h$, in which case smoothing error dominates overall error. First-order consistent methods appear to ensure convergence of the gradient approximation, but do not guarantee global second-order convergence.

In principle it is possible to achieve asymptotic second-order convergence as $h \to 0$ even in standard SPH, if h and $\Delta x/h$ are manipulated together in such a way that discretization and smoothing errors decrease at the same rate. For the ideal case of uniform distribution (Equation (16)), this requires that the relationship $\Delta x/h \propto h^{2/(\beta+2)}$ be maintained throughout refinement. Then, if β is high (in other words, if the kernel is very smooth), Δx can be reduced just a little faster than h. For non-uniform particle spacing, Equation (23) suggests that $\Delta x/h$ should be proportional to h to maintain a constant ratio between the leading terms of the smoothing and discretization error series (under the somewhat simplistic assumption that the non-uniformity parameter δ will be independent of $\Delta x/h$ and h). This scenario is illustrated numerically in Figure 9, showing results of numerical experiments in which h and $\Delta x/h$ were varied together in prescribed relationships on severely non-uniform particle distributions. Near second-order convergence is maintained to very low h/λ if particle spacing varies according to $\Delta x/h \propto h$. Also as Equation (23) predicts, error does not vary with h if $\Delta x/h \propto h^{1/3}$. However, with $\Delta x/h \propto h^{1/10}$ ($\Rightarrow \Delta x \propto h^{11/10}$), divergence is not avoided. This result is contrary to Monaghan's argument [4] that second-order convergence in h can be obtained by decreasing Δx according to $\Delta x/h \propto h^{\varepsilon/(1-\varepsilon)}$ for arbitrarily small ε.

Copyright © 2005 John Wiley & Sons, Ltd.

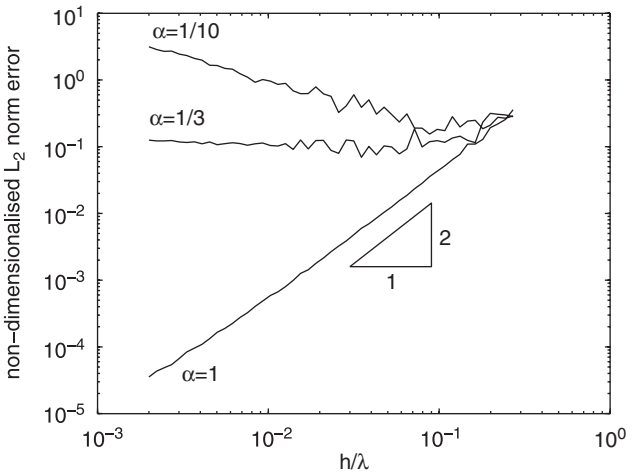

Figure 9. Observed L_2 norm error in estimates of the gradient of $A(x) = A_0 \sin(2\pi x/\lambda)$, for particle spacing perturbation $\sigma/\Delta x = 0.2$, with $\Delta x/h \propto h^{\alpha}$. The $\Delta x/h$ value corresponding to the maximum h value is 0.9 in each case.

Any discussion of accuracy for particle methods is complicated by the availability of two readily adjustable spatial parameters, h and $\Delta x/h$. The standard SPH gradient estimate does not converge globally as smoothing length alone tends to zero. In practice, however, mesh size or smoothing length does not tend to zero, and modellers seek the coarsest and least expensive discretization scale that achieves required accuracy. The pragmatic and successful approach in SPH has been to choose a fixed $\Delta x/h$ which is small enough to ensure good behaviour for the finite range of smoothing length likely to be encountered. This means that the method is operating in the smoothing-limited regime, with negligible discretization effects and second-order error in h. For example, Cleary and Monaghan [25] demonstrated second-order convergence in 2D while varying h by a factor of 4, with fixed $\Delta x/h = 5/6$ (21 particles per kernel support) and uniformly spaced particles. The choice of $\Delta x/h$ must usually be based on judgement and experimentation; values from around 0.7 [14] to 1.0 [6] have been used in engineering applications of SPH. The results presented here indicate that fixed $\Delta x/h$ may often be reliable, but can result in failure of standard SPH, while consistency-corrected methods can restore robustness.

7. CONCLUSIONS

Truncation error in both standard and corrected one-dimensional SPH approximations has been modelled analytically by Taylor series expansions. This direct approach has yielded important insights, confirmed by numerical experiments. In three dimensions, numerical experiments have been carried out along with a limited theoretical analysis, to find that truncation error behaviour is similar in one and three dimensions.

If SPH is viewed as a two-stage method combining integral smoothing with a discrete approximation, it has been shown that discretization effects limit the error as smoothing length h

Copyright © 2005 John Wiley & Sons, Ltd.

is decreased, and conversely, that smoothing error dominates when the ratio of particle spacing to smoothing length, $\Delta x/h$, is small. The smoothness of the kernel and its derivatives at the edges of the compact support has been shown to be an important characteristic when discretization effects dominate and particle spacing is uniform. For non-uniformly spaced particles, SPH behaves in a complex manner. Discretization error can increase as smoothing length is decreased below a critical value.

In first-order consistent methods, on the other hand, error decreases monotonically as smoothing length is reduced, even if particles are unevenly distributed. A first-order consistent method is accurate to second order (in smoothing length) for larger smoothing lengths, and undergoes a transition to first-order accuracy for finer smoothing lengths.

The results of this analysis confirm that the accuracy of particle methods is influenced by particle spacing as well as smoothing length. The role of both parameters must be understood, as attempts to improve resolution by reducing either the smoothing length h or the ratio $\Delta x/h$ alone may be ineffective or even counterproductive. It is likely that the worst-case scenarios described here occur only in extreme circumstances, and indeed there is a long and diverse record of successful applications of standard SPH.

In future work, this analysis will be extended to provide practical guidelines for the selection of h and $\Delta x/h$ values to optimize the balance of accuracy against computational effort, accounting for the compound effects of smoothing length, mean particle spacing, and the non-uniformity of particle spacing. Based on the present work, however, a few preliminary recommendations can be offered for users of standard SPH. A smooth kernel function should be used to reduce discretization error (which becomes significant at large values of $\Delta x/h$) without any increase in the number of particle interactions to be computed. When particles are very unevenly spaced, $\Delta x/h$ should be set low enough to ensure that accuracy is dominated by smoothing effects (a few specific examples for 3D are illustrated in Figure 7). Finally, when adjusting h to reduce error, $\Delta x/h$ must be reduced more rapidly than $h^{1/3}$ to guarantee improvement in accuracy (although convergence over a limited range of h may be achieved without observing this rule).

REFERENCES

1. Lucy LB. A numerical approach to the testing of fission hypothesis. *Astronomical Journal* 1977; **82**:1013–1024.
2. Monaghan JJ, Gingold RA. Smoothed particle hydrodynamics: theory and application to non-spherical stars. *Monthly Notices of the Royal Astronomical Society* 1977; **181**:375–389.
3. Monaghan JJ. Smoothed particle hydrodynamics. *Annual Review of Astronomy and Astrophysics* 1992; **30**: 543–574.
4. Monaghan JJ. New developments in smoothed particle hydrodynamics. In *Meshfree Methods for Partial Differential Equations*, Griebel M, Schweitzer MA (eds), Lecture Notes in Computational Science and Engineering, vol. 26. Springer: Berlin, 2003.
5. Monaghan JJ. Smoothed particle hydrodynamics. *Reports on Progress in Physics* 2005; **68**:1703–1759.
6. Randles PW, Libersky LD. Smoothed particle hydrodynamics: some recent improvements and applications. *Computer Methods in Applied Mechanics and Engineering* 1996; **139**(1–4):375–408.
7. Vignjevic R. Review of development of the smooth particle hydrodynamics (SPH) method. *Sixth Conference on Dynamics and Control of Systems and Structures in Space*, Riomaggiore, Italy, July 2004.
8. Li S, Liu WK. *Meshfree Particle Methods*. Springer: Berlin, 2004.
9. Liu GR, Liu MB. *Smoothed Particle Hydrodynamics*: *A Meshfree Particle Method*. World Scientific: Singapore, 2003.
10. Monaghan JJ. Simulating free surface flows with SPH. *Journal of Computational Physics* 1994; **110**(2): 399–406.

Copyright © 2005 John Wiley & Sons, Ltd.

11. Cummins SJ, Rudman M. An SPH projection method. *Journal of Computational Physics* 1999; **152**(2): 584–607.
12. Ellero M, Serrano M, Español P. On a new incompressible formulation for SPH. In *Meshless 2005*: *Proceedings of the ECCOMAS Thematic Conference on Meshless Methods*, Leitão VMA, Alves CJS, Duarte CA (eds). DM-IST: Lisbon, 2005.
13. Lastiwka M, Basa M, Quinlan NJ. Incompressible smoothed particle hydrodynamics using a Clebsch–Weber decomposition. In *Meshless 2005*: *Proceedings of the ECCOMAS Thematic Conference on Meshless Methods*, Leitão VMA, Alves CJS, Duarte CA (eds). DM-IST: Lisbon, 2005.
14. Takeda H, Miyama SM, Sekiya M. Numerical simulation of viscous flow by smoothed particle hydrodynamics. *Progress of Theoretical Physics* 1999; **92**(5):939–960.
15. Sigalotti LG, Klapp J, Sira E, Melean Y, Hasmy A. SPH simulations of time-dependent Poiseuille flow at low Reynolds numbers. *Journal of Computational Physics* 2003; **191**(2):622–639.
16. Basa M, Lastiwka M, Quinlan NJ. Poiseuille flow with SPH: effects of viscosity and boundary implementation. In *Meshless 2005*: *Proceedings of the ECCOMAS Thematic Conference on Meshless Methods*, Leitão VMA, Alves CJS, Duarte CA (eds). DM-IST: Lisbon, 2005.
17. Violeau D. One- and two-equations turbulent closures for smoothed particle hydrodynamics. In *Hydroinformatics*: *Proceedings of the 6th International Conference*, Liong S-Y, Phoon K-K, Babovic V (eds). World Scientific: Singapore, 2004.
18. Issa R. Numerical assessment of the smoothed particle hydrodynamics gridless method for incompressible flows and its extension to turbulent flows. *Ph.D. Thesis*, University of Manchester, 2005.
19. Liu WK, Jun S, Zhang YF. Reproducing kernel particle methods. *International Journal for Numerical Methods in Fluids* 1995; **20**:1081–1106.
20. Dilts GA. Moving-least-squares-particle-hydrodynamics—I. Consistency and stability. *International Journal for Numerical Methods in Engineering* 1999; **44**(8):1115–1155.
21. Bonet J, Lok T-SL. Variational and momentum preservation aspects of smooth particle hydrodynamic formulations. *Computer Methods in Applied Mechanics and Engineering* 1999; **180**(1–2):97–115.
22. Liu MB, Liu GR, Lam KY. Constructing smoothing functions in smoothed particle hydrodynamics with applications. *Journal of Computational and Applied Mathematics* 2003; **155**(2):263–284.
23. Meglicki Z. Verification and accuracy of smoothed particle magnetohydrodynamics. *Computer Physics Communications* 1993; **81**(1–2):91–104.
24. Fulk DA, Quinn DW. An analysis of 1-D smoothed particle hydrodynamics kernels. *Journal of Computational Physics* 1996; **126**(1):165–180.
25. Cleary PW, Monaghan JJ. Conduction modelling using smoothed particle hydrodynamics. *Journal of Computational Physics* 1999; **148**(1):227–264.
26. Han W, Meng X. Error analysis of the reproducing kernel particle method. *Computer Methods in Applied Mechanics and Engineering* 2001; **190**(46–47):6157–6181.
27. Monaghan JJ, Lattanzio JC. A refined particle method for astrophysical problems. *Astronomy and Astrophysics* 1985; **149**(1):135–143.
28. Belytschko T, Krongauz Y, Organ D, Fleming M, Krysl P. Meshless methods: an overview and recent developments. *Computer Methods in Applied Mechanics and Engineering* 1996; **139**(1–4):3–47.
29. Ralston A. *A First Course in Numerical Analysis*. McGraw-Hill: New York, 1965.
30. Yakowitz S, Krimmel JE, Szidarovszky F. Weighted Monte Carlo integration. *SIAM Journal on Numerical Analysis* 1978; **15**(6):1289–1300.

Copyright © 2005 John Wiley & Sons, Ltd.